SANDIA REPORT

SAND87—1753 • UC—62B
Unlimited Release
Printed December 1987

Oxidation/Sulfidation of Materials in an $SO_3/SO_2/O_2$ Thermochemical-Transport, Distributed-Receiver, Solar-Energy System

Final Report

L. J. Weirick

Prepared by
Sandia National Laboratories
Albuquerque, New Mexico 87185 and Livermore, California 94550
for the United States Department of Energy
under Contract DE-AC04-76DP00789

Issued by Sandia National Laboratories, operated for the United States Department of Energy by Sandia Corporation.

Printed in the United States of America
Available from
National Technical Information Service
U.S. Department of Commerce
5285 Port Royal Road
Springfield, VA 22161

NTIS price codes
Printed copy: A02
Microfiche copy: A01

SAND87–1753
Unlimited Release
Printed December 1987

Distribution
Category UC–62B

Oxidation/Sulfidation of Materials in an $SO_3/SO_2/O_2$ Thermochemical-Transport, Distributed-Receiver, Solar-Energy System

Final Report

L. J. Weirick
Explosive Projects and Diagnostics Division
Sandia National Laboratories
Albuquerque, NM 87185

Abstract

Metals for potential use in the dissociator and the synthesizer reactors of a distributed solar-receiver, thermochemical-transport loop using $SO_3/SO_2/O_2$ molecular chemistry were tested in SO_3 gas at 500°C and 900°C, respectively, for periods up to 8 weeks and in a cyclic-temperature mode from 200°C to 900°C, representing the diurnal solar cycle, for 35 days. They included iron-base, nickel-base, and cobalt-base superalloys. Weight-gain measurements were used to determine the oxidation/sulfidation kinetics. Electron-microprobe analysis identified any possible penetration of oxygen and sulfur into the metal and the formation of internal oxides and sulfides. Selected iron-base, nickel-base, and cobalt-base alloys look promising as candidates for the synthesizer reactor which operates at ~500°C. The most promising candidate for the dissociator reactor that operates above 900°C is Kanthal A-1, which contains sufficient quantities of both aluminum and chromium alloying additions to be an alumina and chromia former.

Acknowledgment

The author wishes to acknowledge the assistance of the following people: C. J. Greenholt, Corrosion Division, for constructing the experimental systems, preparing the coupons, and performing the tests, M. E. McAllaster, Electron Optics and X-Ray Analysis Division, for the metallographic examination, and R. E. Semarge, Electron Optics and X-Ray Analysis Division, for the electron-microprobe analyses.

Contents

Figures

Tables

Summary

From a corrosion standpoint, selected iron-base, nickel-base, and cobalt-base superalloys offer promise as metal candidates to be used in the synthesizer reactor of a distributed solar-receiver, thermochemical-transport system. Only Kanthal A-1 looked promising as a candidate for the dissociator reactor.

Oxidation/Sulfidation of Materials in an $SO_3/SO_2/O_2$ Thermochemical-Transport, Distributed-Receiver, Solar-Energy System

Final Report

Introduction

Distributed-Receiver, Thermochemical-Transport System

Thermochemical-transport systems are being considered for distributed receivers. One possible system involves gaseous SO_3, SO_2, and O_2 as the transport media. Figure 1 shows a schematic of the thermochemical-transport system. One side of the loop shows the parabolic dish that concentrates the solar energy into a cavity with piping containing SO_3 gas. At temperatures above 900°C, the SO_3 is passed over a platinum-coated, alumina catalyst and is dissociated into SO_2 and free oxygen. This part of the system is termed the "dissociator." The hot SO_2 and O_2 pass through a heat exchanger which cools the gas to ~150°C to minimize the cost of insulation and thermal losses during transfer. The cool gas is piped to a chemical reactor which contains a platinum catalyst on alumina beads. In this reactor, called a synthesizer, the gas is heated to ~500°C where the SO_2 and O_2 are chemically combined in an exothermic reaction to form the SO_3 product. The heat generated by this exothermic reaction can be used to produce steam for process heat as well as to run turbines and generate electricity. The SO_3 gas is cooled and transported back to the dissociator.

In considering materials for the system design, the primary importance to this part of the program is oxidation and sulfidation of the materials of construction, particularly for the reactors.

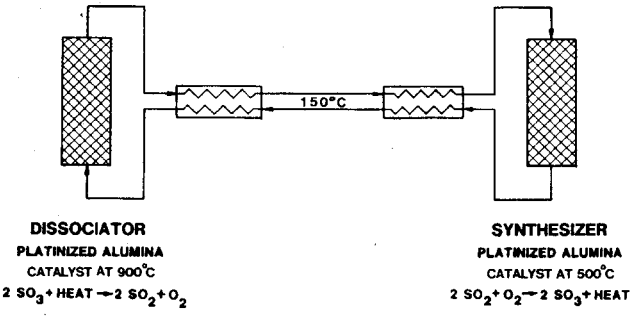

Figure 1. Schematic of thermochemical-transport system

Program Plan

The organizational guide used in this program separated the objectives and effort into segments defined by temperature and gas composition. Five segments were defined: two temperatures (500°C and 900°C) and two gas compositions (SO_2/O_2 and SO_3) plus a cyclic-temperature mode from 200°C to 900°C. One published report, SAND85-0757[1], documented the results of tests between the material candidates and SO_2/O_2 mixtures at 500°C and 900°C. A second report, SAND85-2091[2], covered testing in SO_3 gas at temperatures of 500°C and 900°C for test periods up to 4 weeks. This report discusses the test results from cyclic-temperature testing and compares them with new results from tests done for 8 weeks at 500°C and 900°C, respectively, in SO_3.

Experimental Procedure

Material Candidates

Table 1 lists the material candidates and their chemical compositions. The list includes candidates from the families of iron-base, nickel-base, and cobalt-base superalloys. Particular notice should be made of three alloying additions in this table.

1. All of the alloys have at least 15% chromium, which is considered the minimum amount to be a chromia-former in an oxidizing environment. Most alloys contain ~20% to be assured this minimum of 15% is available in solid solution to preferentially react with oxygen in forming a protective chromia scale.
2. RA 330 has an alloying addition of ~2% silicon, which is a sufficient amount to produce a complete silica outer scale. This scale should increase the oxidation resistance to a considerable degree over that of Incoloy 800 which, other than the silicon, has a similar composition to RA 330.
3. Kanthal A-1, Nimonic 105, and Cabot 214 have an alloying addition of ~5% aluminum, which is a sufficient amount to produce a complete alumina outer scale. Alumina generally increases the protectiveness of a scale for both oxidation and sulfidation resistance.

Table 1. Metal Candidate Compositions

Metal	Chemical Composition (wt. %)
Incoloy 800	21Cr, 32.5Ni, 0.4Ti, 0.4A1, 46Fe
RA 330	19Cr, 36Ni, *2Si*, 0.2Cu, 43Fe
Kanthal A-1	22Cr, *5.5A1*, 0.5Co, 72Fe
Inconel 625	22Cr, 9Mo, 3.6(Nb+Ta), 2.5Fe, 0.2Ti, 0.2A1, 62Ni
Hastelloy X	22Cr, 18Fe, 9Mo, 2Co, 1W, 45Ni
Nimonic 105	15Cr, 20Co, 5Mo, *5A1*, 2Ti, 54Ni
Cabot 214	16Cr, *4.5A1*, 2.5Fe, 2Co, 0.5Mn, 0.2Si, 0.02Y, 75Ni
Haynes 188	22Cr, 22Ni, 14W, 3Fe, 36Co
MP35N	20Cr, 35Ni, 10Mo, 35Co

Constant-Temperature Tests

A schematic of the system used to expose coupons of the metal candidates to SO_3 mixtures at constant temperature is shown in Figure 2. Nine coupons of materials listed in Table 1 were exposed simultaneously to SO_3 gas at 500°C and 900°C, respectively, for up to 8 weeks. The dimensions of the coupons were generally 2.54 × 2.54 × 0.15 cm (1 × 1 × 1/16 in.) and weighed ~7 g, initially, dependent upon material density. The surface finish was specified as a 600-grit SiC polish followed by an acetone and alcohol rinse. After an initial weight determination, the coupons were suspended from a quartz holder placed within the furnace hot zone. The gas-flow rate for SO_3 was chosen as 10 cc/min. The flow rate was controlled initially by a Matheson flow controller to an accuracy of ±0.1 cc/min. However, with time the elastomer seals in the flow sensor were attacked by the SO_3 and this technique was abandoned and a stainless-steel needle valve replaced the flow controller. At predetermined times, the coupons were removed and weighed on a Mettler balance to an accuracy of ±0.01 mg. Specific area weight gains were calculated from the weight-change data.

Cyclic-Temperature Tests

A schematic of the apparatus used for the cyclic-temperature testing in SO_3 is shown in Figure 3. The test samples were 1-cm-dia, 5-cm-long tubes with 0.63-cm threads tapped in each end. The sample tubes were joined together using tubular studs fabricated from 316 SS. Four samples were tested in each test. The materials subjected to the cyclic-temperature tests were the same as those listed in Table 1, with the deletion of Incoloy 800 and MP35N. SO_3 was passed through the inside and air was passed over the outside of the metal tubes, thus simulating an actual field installation. A parabolic, clamshell, radiant-heating chamber was used to heat the samples because of the rapid heating and cooling characteristics. The temperature cycle used is shown schematically in Figure 4 and represented the temperature profile of a dissociator reactor during a solar day. The cycle duration was 10 hr total. The tests were run for 85 cycles/35 days.

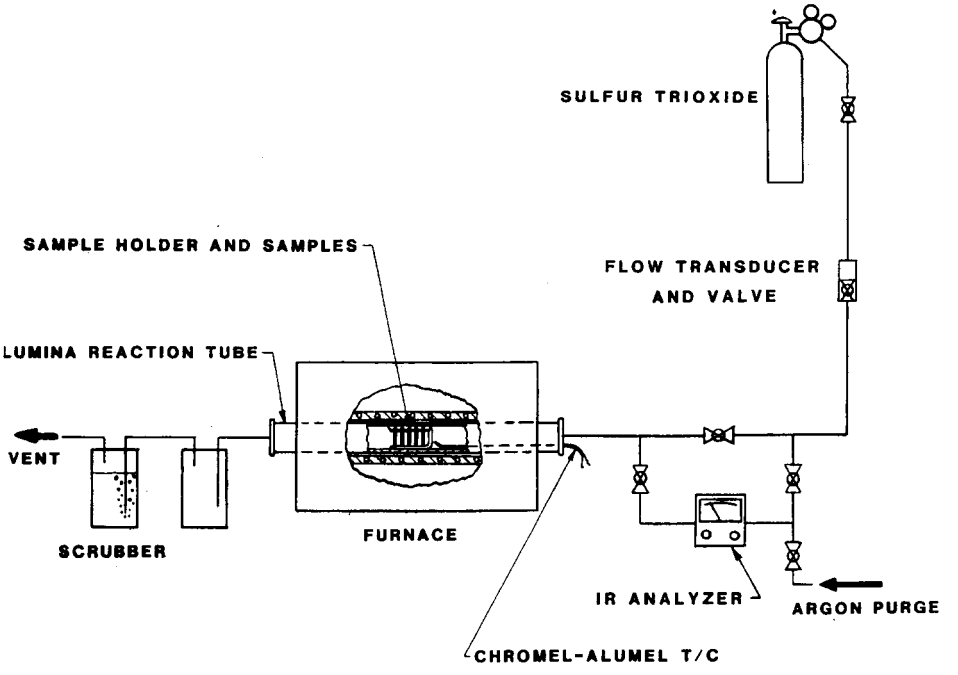

Figure 2. Schematic of constant-temperature, oxidation/sulfidation test system

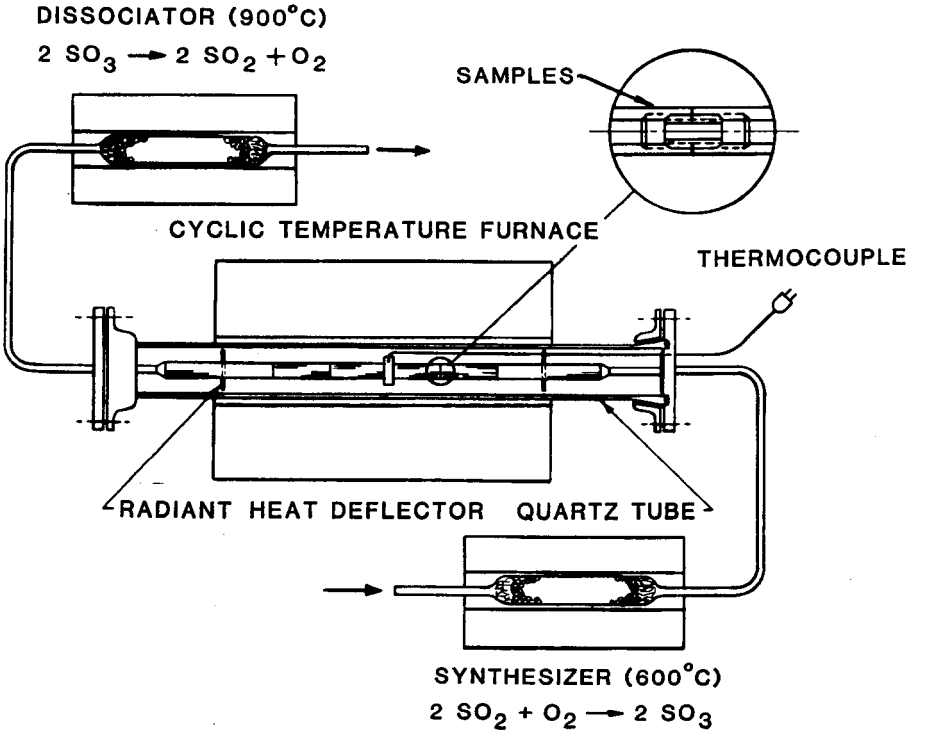

Figure 3. Schematic of cyclic-temperature, oxidation/sulfidation test system

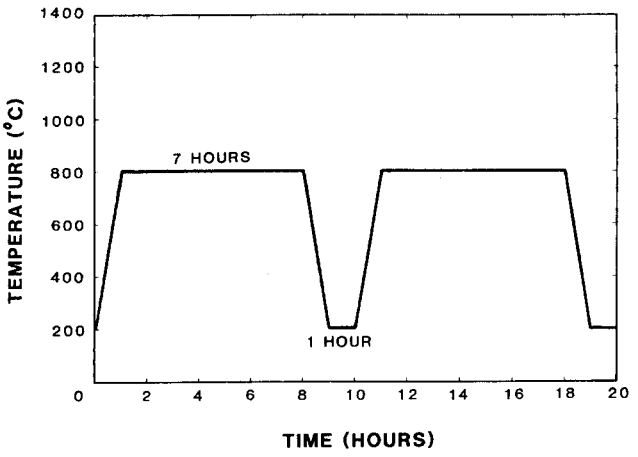

Figure 4. Schematic of cyclic-temperature/time profile

Analysis Techniques

Macrophotography was used to record the changes in appearance of the coupons or tubes with increasing exposure time to the SO_3 gas. The coupons or tubes were overplated with nickel to protect the corrosion scales during subsequent handling. They were individually cut, mounted, polished, and prepared for metallographic examination. These same specimens were also analyzed in the electron microprobe where any internal species, in addition to the external corrosion scales, were identified.

Results

500°C

The weight-change data taken on two sets of coupons exposed to SO_3 gas at 500°C for 8 weeks are shown in Table 2. A number of observations can be made from this data.

- The weight-loss data for a specific alloy, as well as relative to the other alloys, had good reproducibility.
- The nickel-base alloys such as Hastelloy X and Inconel 625 (those not containing an appreciable aluminum addition) were not very resistant to SO_3.
- The cobalt-base alloys, MP35N and Haynes 188 exhibited resistance similar to the nickel-base alloys.
- The iron-base alloys had varying degrees of resistance, depending on the composition. Incoloy 800 had a resistance similar to the nickel-base and cobalt-base alloys. RA 330, which contains silicon, had good resistance at this temperature; Kanthal A-1, which also contains aluminum, showed the most resistance of the set.
- Nimonic 105 and Cabot 214, which contain aluminum and chromium, also exhibited good resistance at this temperature.

Table 2. Weight Gains of Coupons Tested at 500°C for 8 Weeks (mg/cm²)

Metal	Test 1	Test 2
Incoloy 800	0.84	0.28*
RA 330	0.16	0.12
Kanthal A-1	0.05	0.05
Inconel 625	0.84	0.88
Hastelloy X	0.82	1.10
Nimonic 105	0.28	0.36
Cabot 214	0.24	0.11
Haynes 188	1.06	0.81
MP35N	0.68*	1.28

*Oxide not adherent, spalled from coupon.

Metallographic examination and electron-microprobe analysis gave no evidence of any grain-boundary penetration of oxygen or sulfur with subsequent internal oxide or sulfide formation for any of the materials tested. Figure 5 shows a set of micrographs taken using the electron microprobe for the Haynes 188 coupon tested at 500°C for 8 weeks in SO_3. This set is representative of all the materials tested under these conditions. No evidence of internal penetration by oxygen or sulfur is seen. The micrographs show an external oxide scale, primarily of chromia, and sulfur also is associated with this scale.

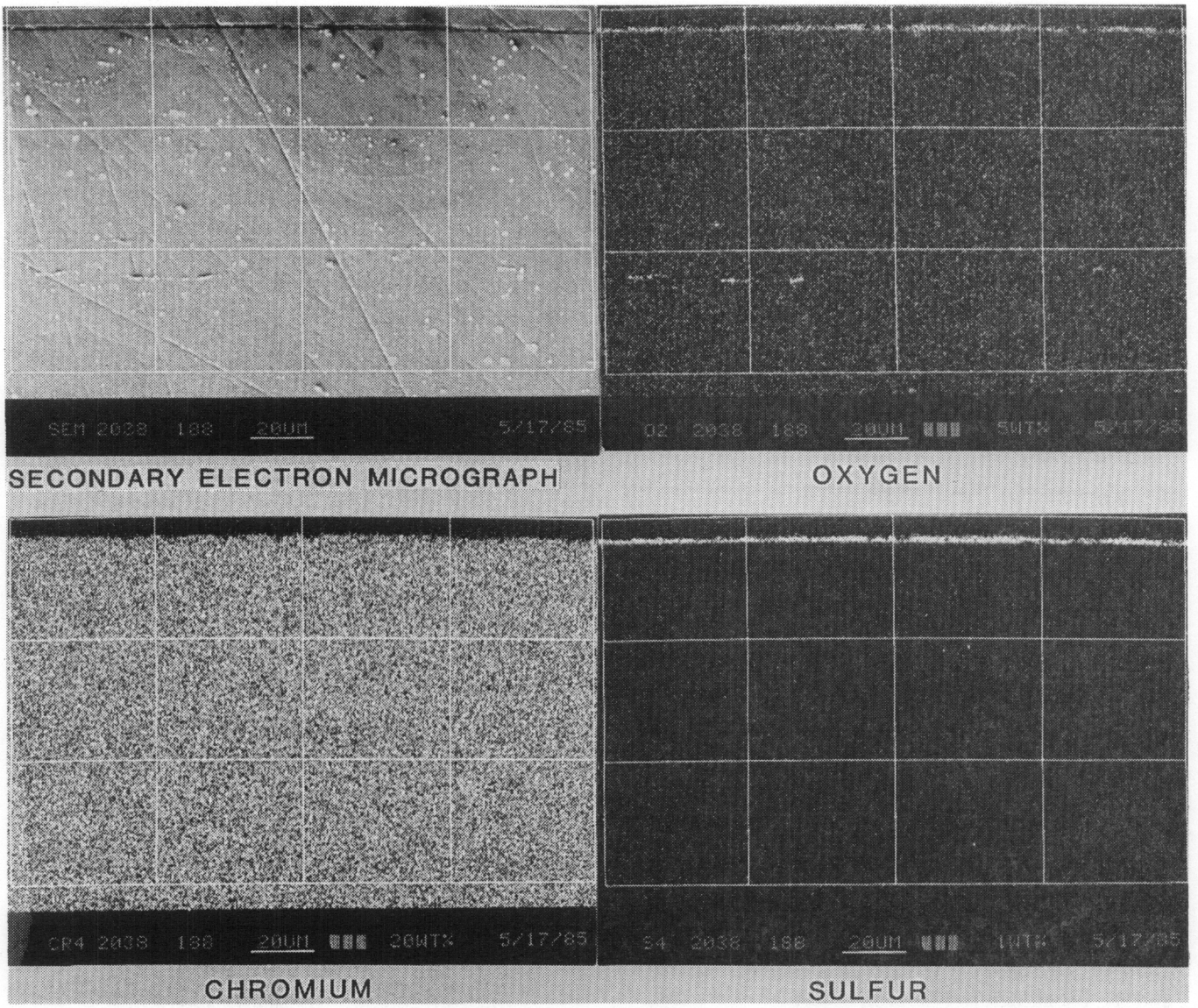

Figure 5. Elemental distribution map for Haynes 188, tested at 500°C

900°C

Table 3 lists the weight-change data taken for a set of nine coupons tested at 900°C in the SO_3 gas for 8 weeks. These results generally agreed with the results from the tests performed at 500°C with respect to the relative performance of an alloy. The iron-base and nickel-base materials performed equally poorly, when the alloying addition of aluminum was absent. The cobalt-base alloys and nickel-base alloys containing aluminum, Nimonic 105 and Cabot 214, formed more adherent and protective scales. However, they exhibited significant weight gains. Kanthal A-1 again showed the best resistance of this group.

Table 3. Weight Gains of Coupons Tested at 900°C for 8 Weeks (mg/cm²)

Metal	Weight Gain
Incoloy 800	1.686*
RA 330	−0.133*
Kanthal A-1	0.421
Inconel 625	1.728
Hastelloy X	−3.489*
Nimonic 105	2.277
Cabot 214	1.378
Haynes 188	1.588
MP35N	1.584

*Oxide not adherent, spalled from coupon

The set of coupons tested at 900°C was examined metallographically and analyzed using an electron microprobe. Figures 6 and 7 give examples of these analyses. The results for Kanthal are shown in Figure 7. The results shown in Figure 6 for Incoloy 800 are representative of the remainder of the metal alloys tested. All of these examples are from coupons exposed at 900°C for 8 weeks. A number of observations apply to both sets. First, the photographs labeled Figures 6a and 7a Scanning Electron Microscope (SEM) were taken in the electron microprobe using secondary electron-emission techniques. The result is a micrograph similar to that received in a standard SEM. These micrographs show the outer corrosion scales and the presence of any internal oxides and sulfides. Second, the photographs labeled Figures 6e and 7e backscattered-electron (BSE) were taken in the electron microprobe using BSE techniques. These micrographs clearly show the presence of internal oxides and sulfides. Third, the remainder of the photographs in each set are elemental distribution maps (EDM) of a particular element covering the same area of the sample shown in the secondary electron micrograph SEM and the BSE micrograph. In particular, the EDMs to the right of the SEM micrographs are for oxygen (Figures 6b and 7b) and the EDMs to the right of the BSE micrographs are for sulfur (Figures 6f and 7f), respectively. The other photographs on the page with that of oxygen (Figures 6c, 6d, 7c, and 7d) show the correspondence of those particular elements with oxygen, such as chromium, aluminum, and silicon. Similarly, those on the page with sulfur (Figures 6g, 6h, 7g, and 7h) show the correspondence of those particular elements with sulfur, such as manganese and titanium. Fourth, manganese and titanium were associated with both oxygen and sulfur, in spite of their EDM placed with that for sulfur. Fifth, the EDM photos identify the outer corrosion scales as having a composition containing chromium, manganese, oxygen and, when applicable, aluminum and titanium. Sixth, the EDM photos identify the penetration down the grain boundaries as an oxide. The oxygen was usually associated with aluminum, but in its absence, silicon. Sulfur, with the exception of MP35N and Nimonic 105, appeared not to be associated with this grain-boundary penetration. Seventh, when sulfur is present, it is associated with a band of internal precipitates observed below the grain-boundary oxide penetration. Manganese and titanium are associated with these internal sulfides.

The results from the Incoloy 800 coupon are shown in Figure 6. These results represent those observed for all of the alloys tested except Kanthal. These results agree with the general observations outlined above. In summary:

- the outer oxide scales are composed primarily of chromium with some manganese, aluminum, titanium, and silicon,
- the grain boundaries have been penetrated near the surface by oxygen with subsequent oxidation of aluminum to form alumina (for RA 330 the grain-boundary oxide was identified as silica),
- internal sulfides have formed in a zone beyond the grain-boundary penetration, and
- these sulfides are a mix of interspersed manganese and titanium sulfides.

The results from the Kanthal A-1 coupon are shown in Figure 7. These results are significantly different from the other alloys. The outer scale was composed of a complete and adherent layer of alumina at the metal/scale interface and an outer layer of chromia. No evidence of oxygen penetration down grain boundaries nor internal oxide formation was seen. A zone of sulfides of titanium or manganese was not observed.

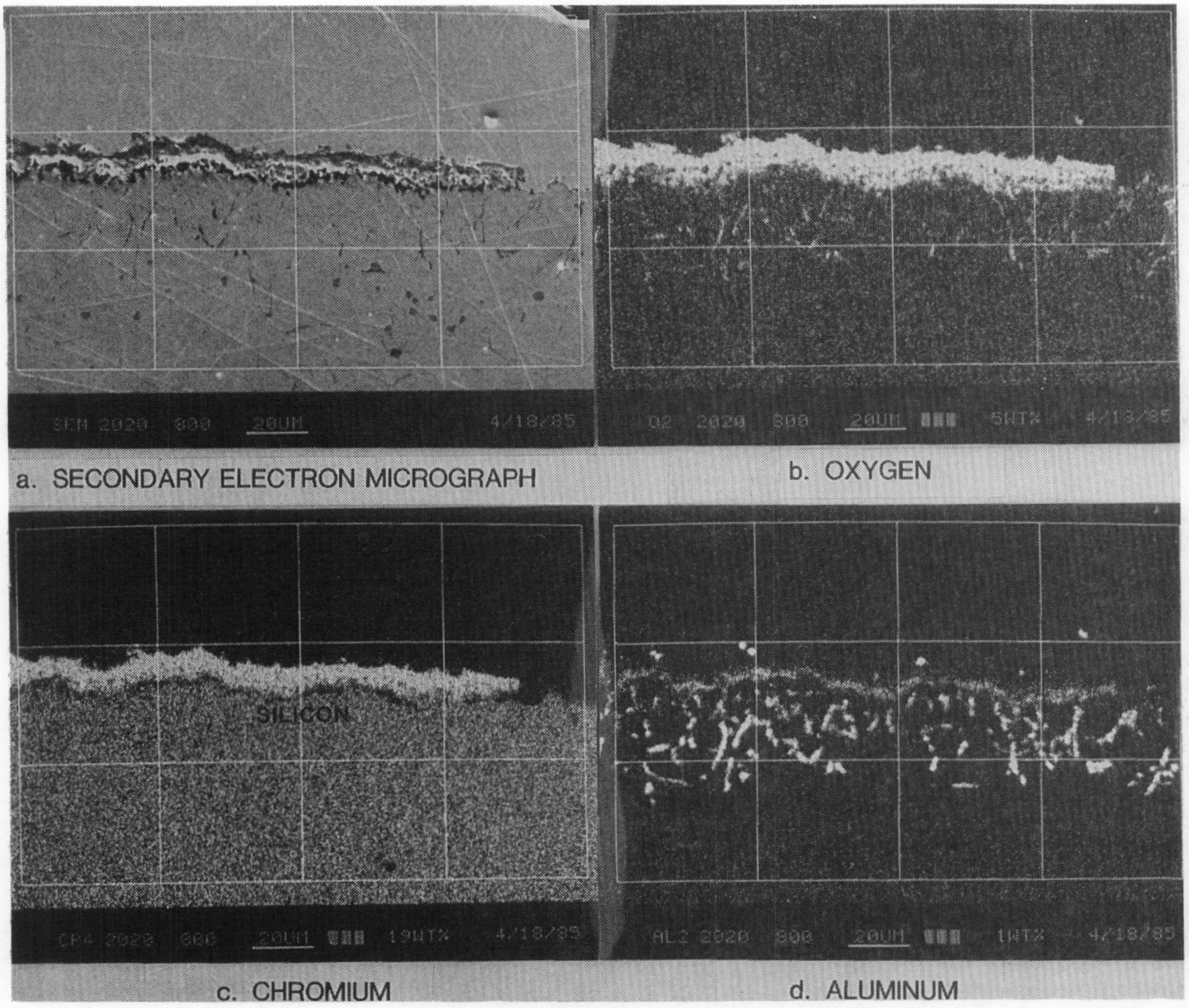

Figure 6. Elemental distribution map for Incoloy 800, tested at 900°C

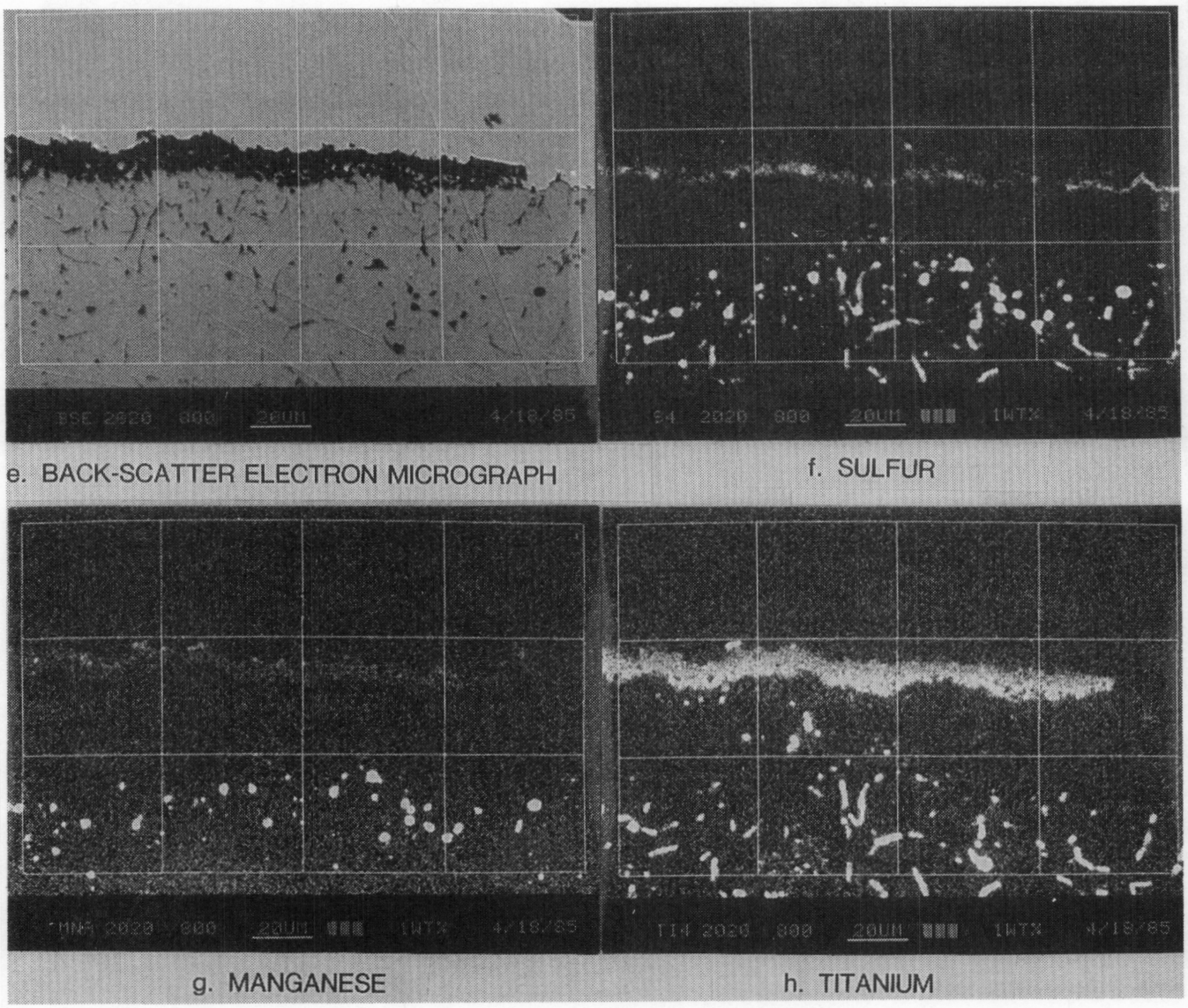

Figure 6. (concluded)

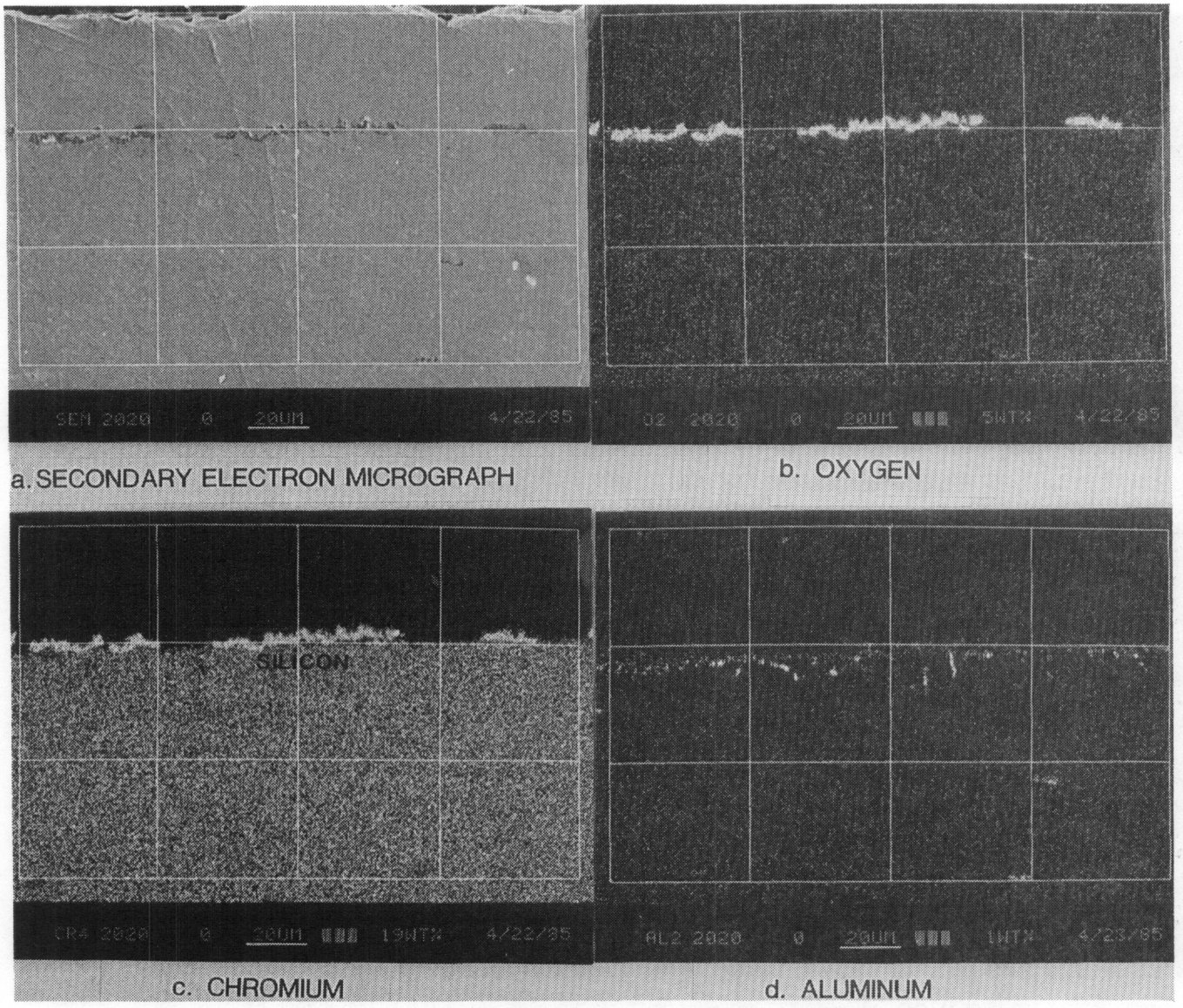

Figure 7. Elemental distribution map for Kanthal A-1, tested at 900°C

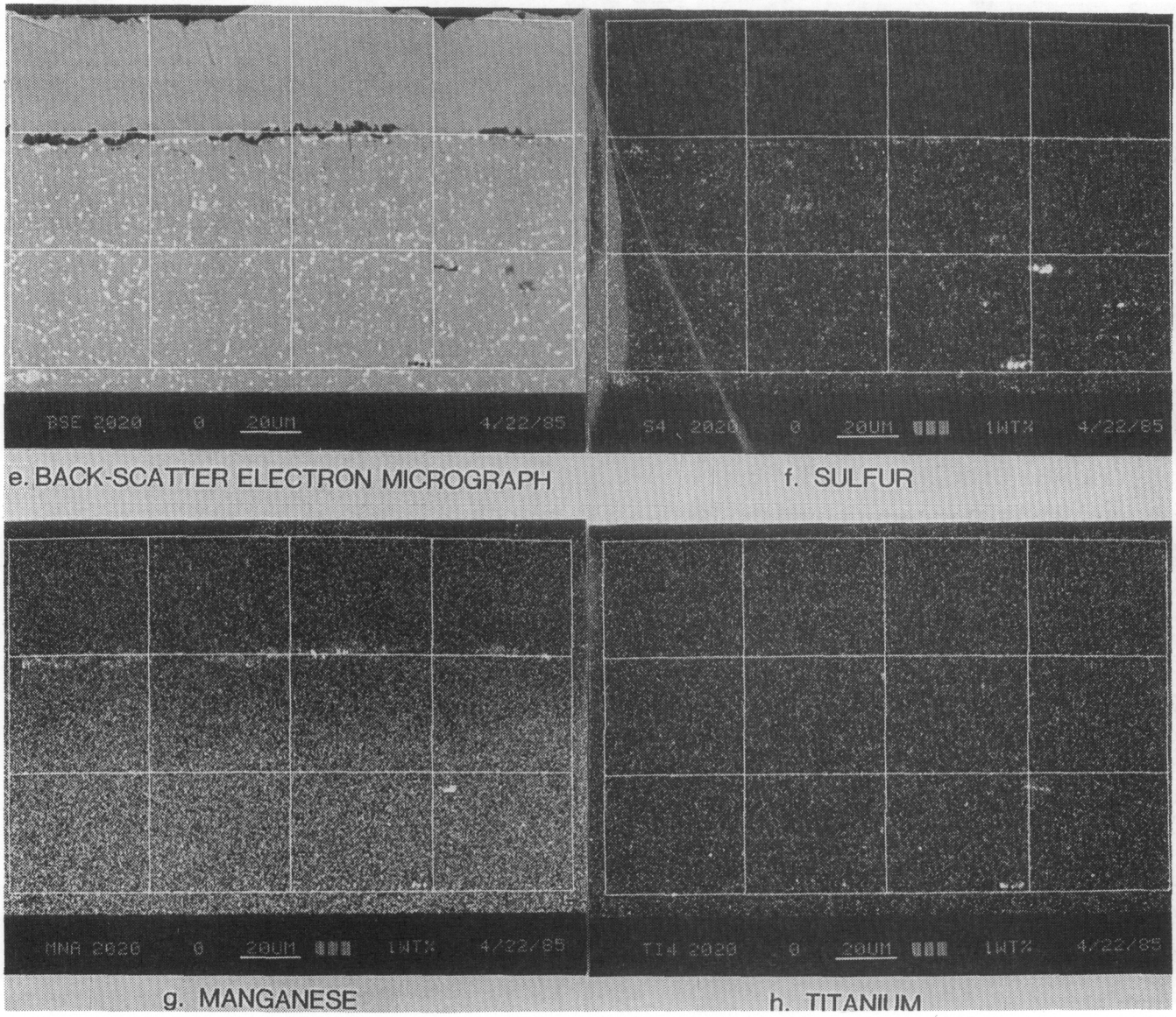

Figure 7. (concluded)

Cyclic Temperature

The external appearance of the tubes after cyclic-temperature testing for 35 days is shown in Figure 8. Although the experimental design of this test was to expose these outer surfaces to air alone, they were exposed to a small partial pressure of sulfur, in addition to oxygen, caused by a small leakage of SO_3 from the inner cavity at the tube joints. All of these alloys have been specifically designed for resistance to oxidation at high temperatures. Kanthal A-1, Nimonic 105 and Inconel 625 had the best appearance, showing no appreciable reaction-scale formation. The cobalt-base alloy, Haynes 188, formed a thin "tarnish" film that detached in some areas. The three other alloys tested, RA 330, Hastelloy X, and Cabot 214, reacted and formed thick corrosion scales.

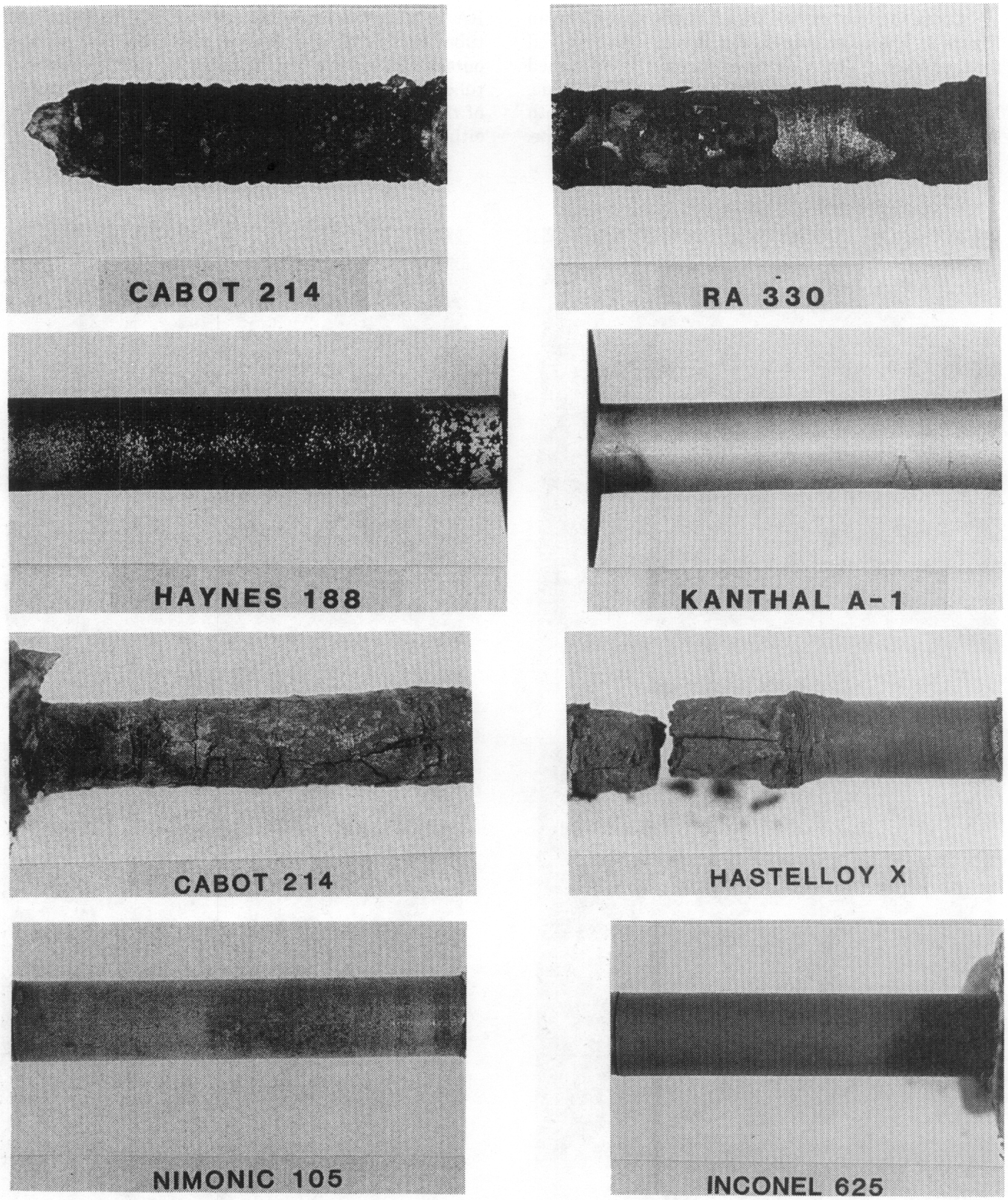

Figure 8. External appearance of cyclic-temperature-tested tubes from 200°C to 900°C

Cross sections of the tested tubes are shown in Figure 9. The most graphic result was that observed for the Cabot 214 tube, as it was completely consumed by the oxidants, from both the inside and the outside. Hastelloy X also reacted with the oxidants on both sides, but more extensively on the outside of the tube. RA 330 reacted predominantly on the inside of the tube with SO_3, but showed some reaction on the outside of the tube. The Nimonic 105 and Inconel 625 tubes showed a small reaction with SO_3 on the inside of the tubes. Kanthal A-1 reacted very slightly with either oxidant.

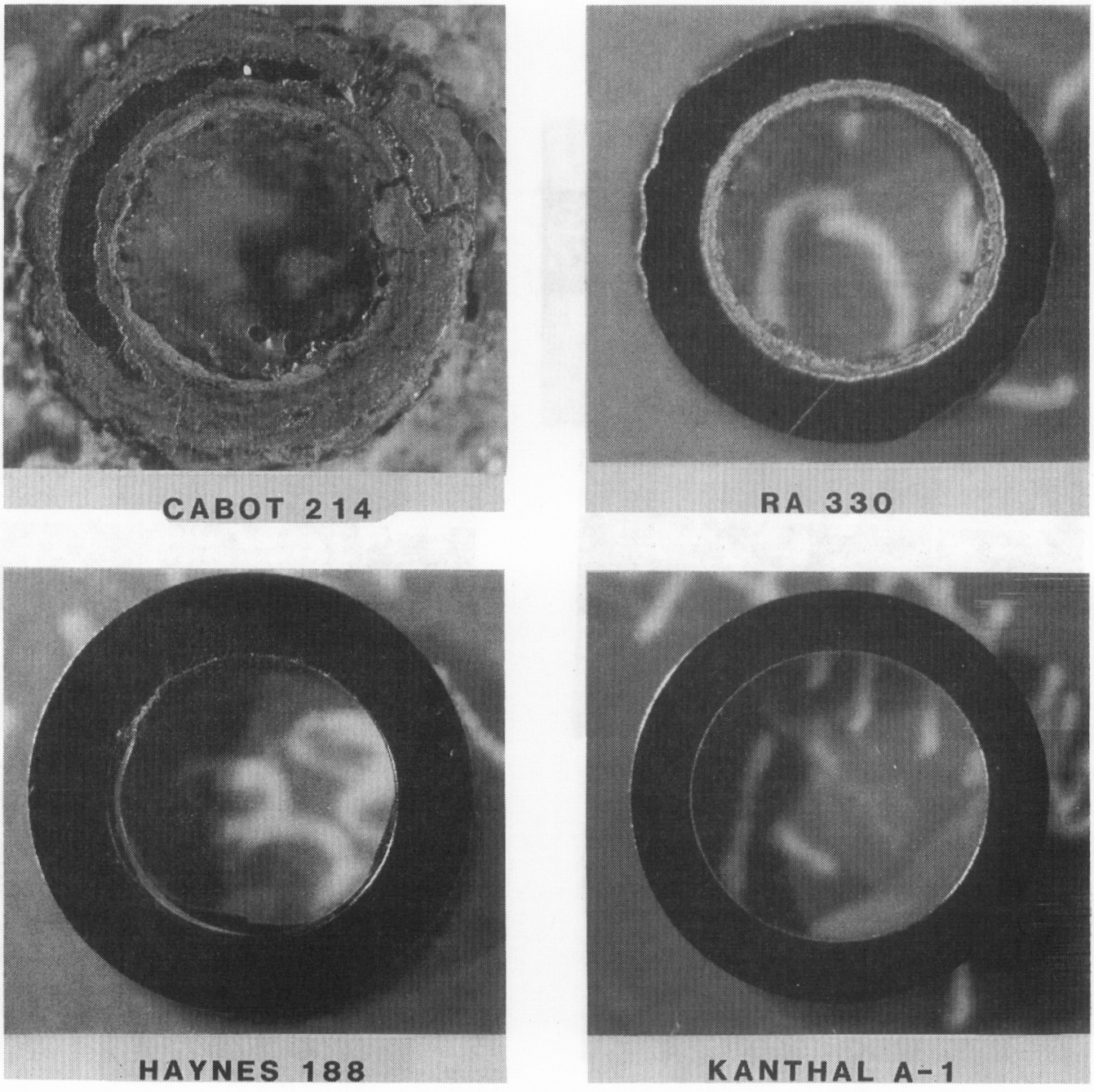

Figure 9. Cross sections of cyclic-temperature-tested tubes

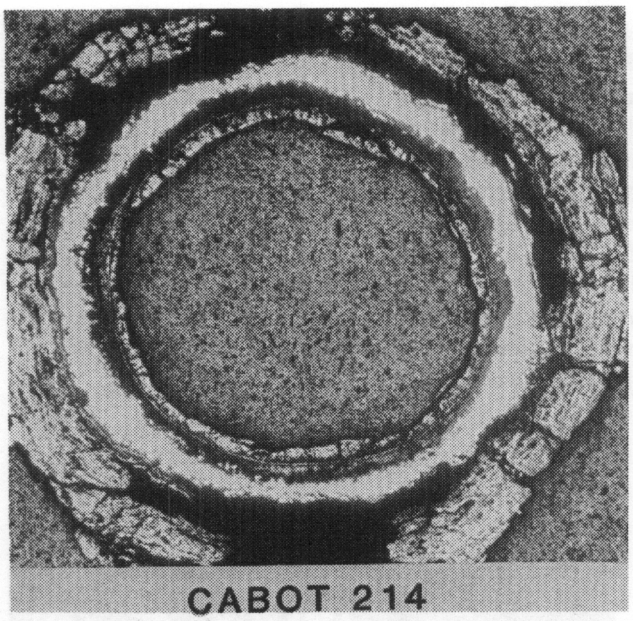

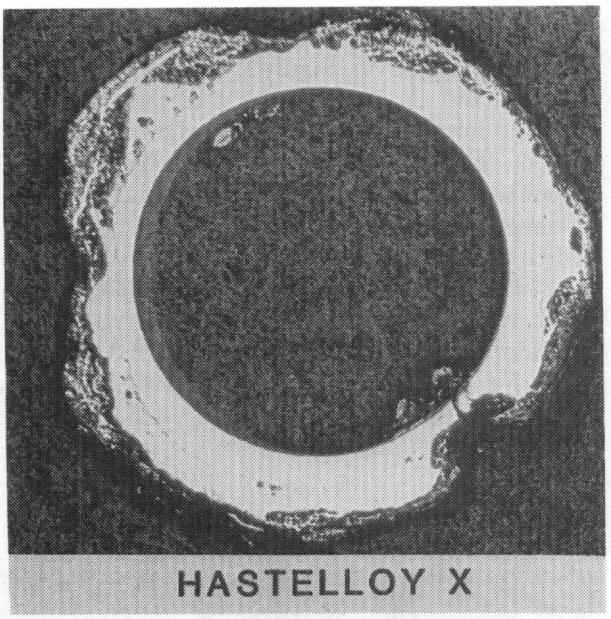

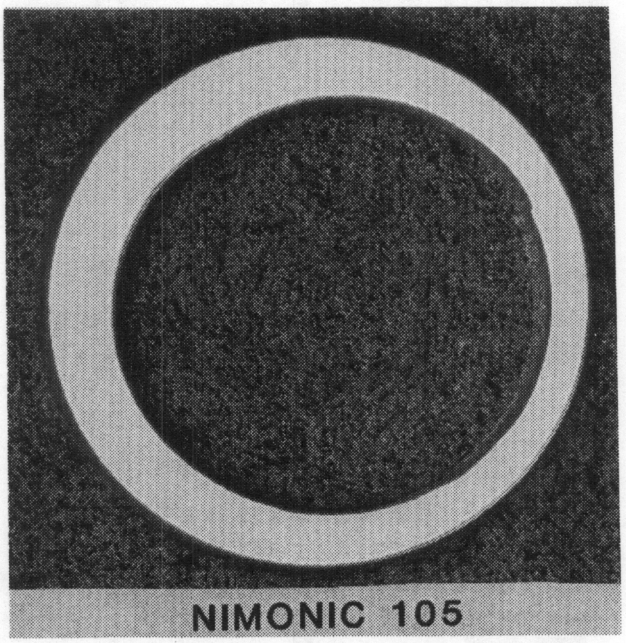

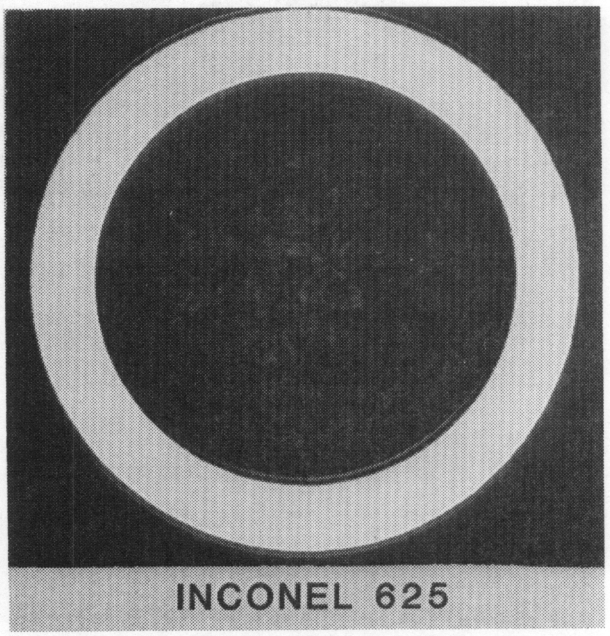

Figure 9. (concluded)

Metallographic cross-sections of the exposed tubes are shown in Figure 10. The metal-oxidant interface and the interior of the metal are shown for both the inner and outer tube surfaces. The appearance of the interfaces of the tubes in these higher-magnification photographs agrees with the results observed in the lower-magnification photographs. In addition to the thick scales formed on the inner surfaces of Cabot 214, Hastelloy X and RA 330, these photographs also show the severe internal oxidation on grain boundaries that had occurred. Although the scales formed on the outer surfaces of these metals were also relatively thick, penetration of oxidants into the metal beneath the surface was not observed. The Nimonic 105 and Inconel 625 tubes formed thin scales on both surfaces and, in addition, formed a thin zone of internal oxides and sulfides beneath the interior surface. Haynes 188 formed a thin reaction scale on the inner surface, exhibited a shallow zone of internal sulfides beneath the inner surface, and formed a very thin tarnish film on the outer surface. Kanthal A-1 showed the most corrosion-resistant appearance. No appreciable corrosion scales nor any interior oxidation or sulfidation were observed for this alloy on either the inner or outer surfaces.

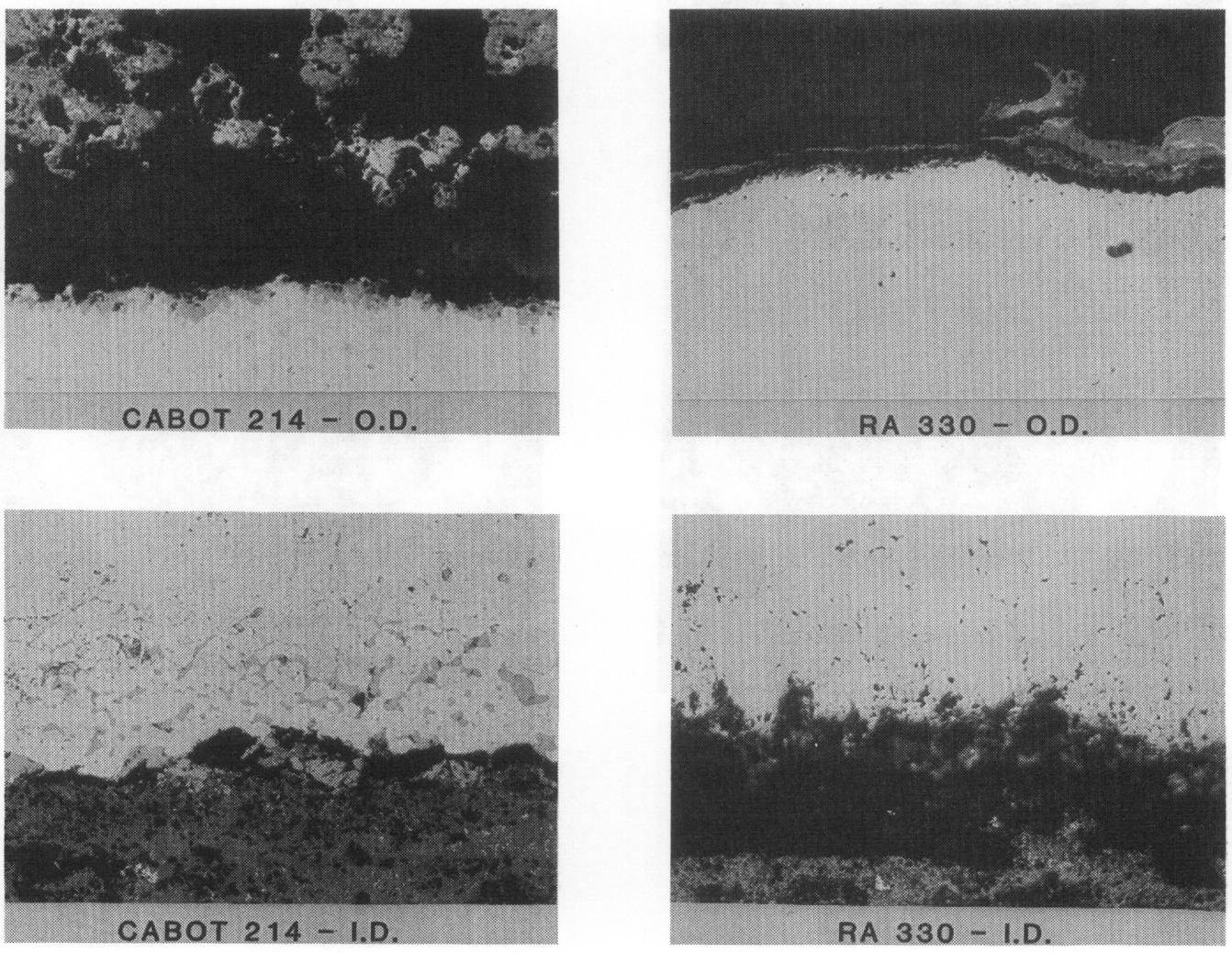

Figure 10. Micrographs of inner and outer interfaces of cyclic-temperature-tested tubes.

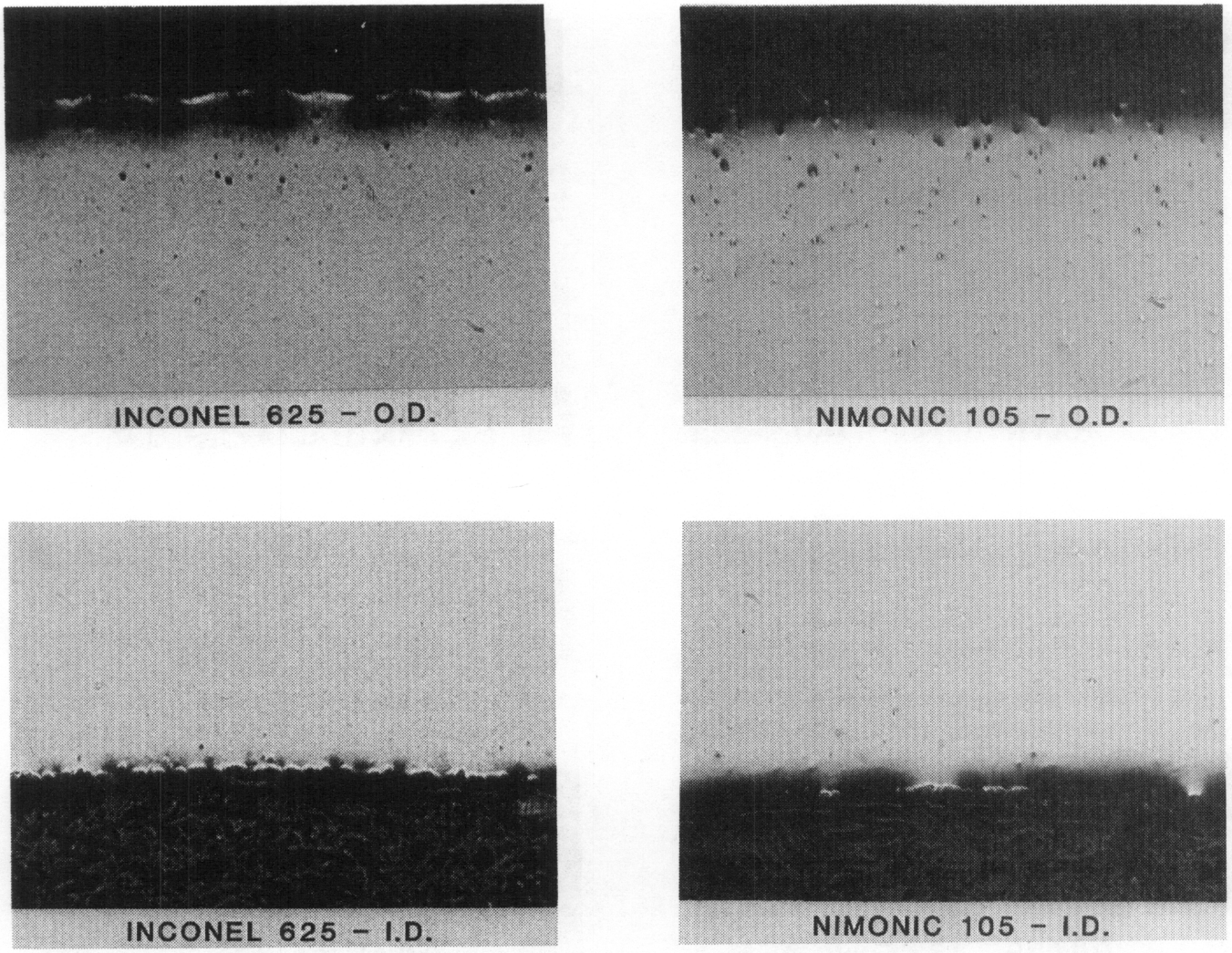

Figure 10. (continued)

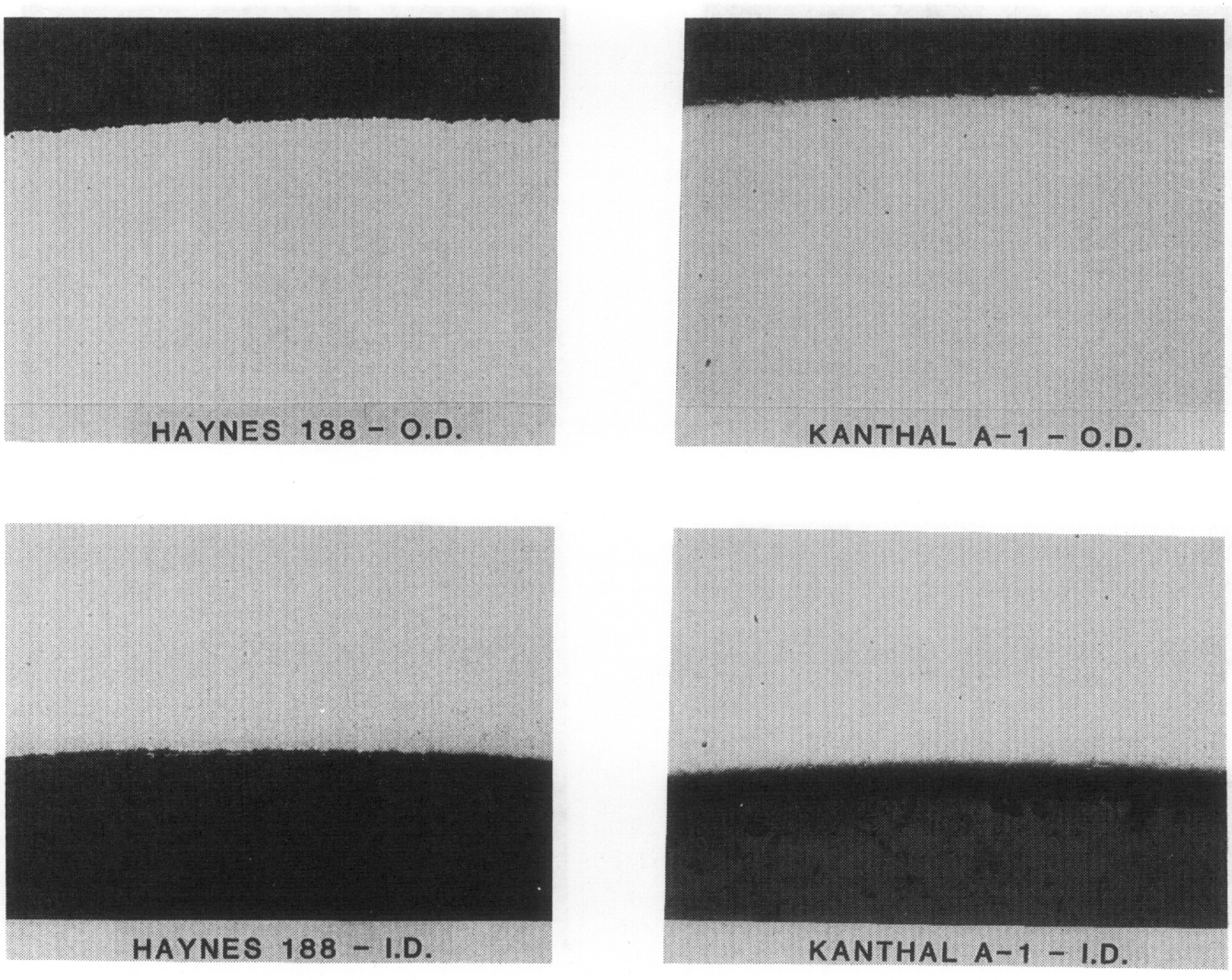

Figure 10. (continued)

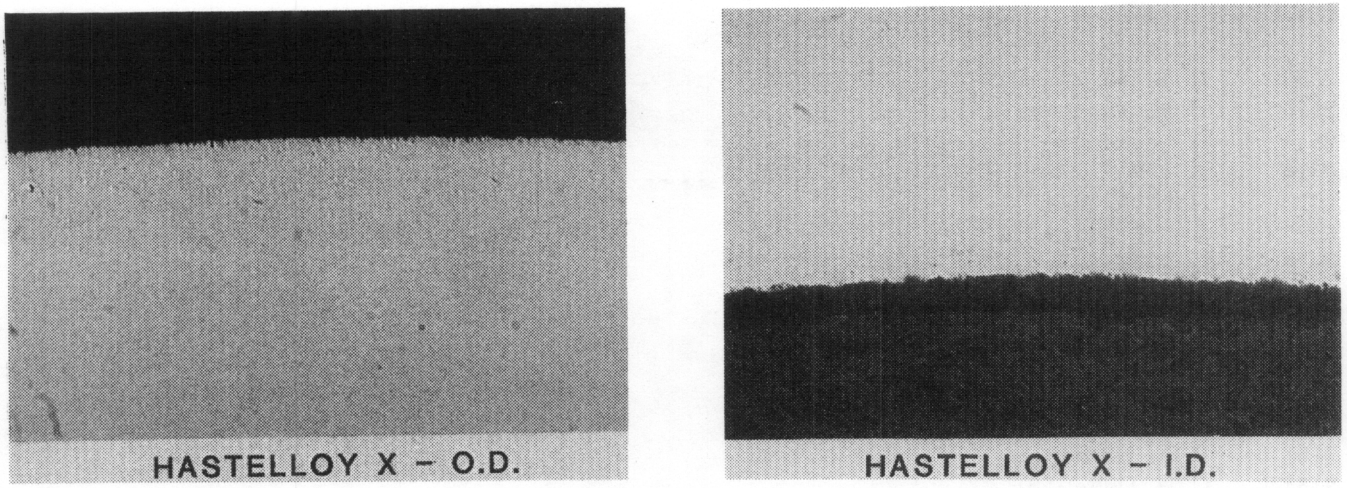

Figure 10. (concluded)

Discussion

Results from these preliminary tests suggest that a material can be qualified for use in solar-distributed, receiver applications. Two observations were encouraging: first, the prevention of grain-boundary penetration of oxygen with subsequent oxide formation by an outer scale of alumina and chromia, such as for Nimonic 105 and Kanthal A-1; and second, the lack of formation of an internal zone of sulfides in Kanthal A-1, which does not contain titanium or manganese.

Although the cobalt-base superalloys showed some signs of oxygen penetration at the grain boundaries and subsequent internal oxide formation, it was not extensive. However, the formation of grain-boundary oxides in the cobalt-base superalloys causes serious concerns about the suitability of these candidates in sulfurous-oxide environments. These subsurface formations, particularly at grain boundaries, can seriously degrade the mechanical strength of the material and lead to premature failure. Failure phenomena such as stress-corrosion-cracking, fatigue, and corrosion-fatigue are made more probable in harsh environments when grain-boundary damage occurs.

Another result that was not encouraging was the consistent presence of an internal sulfide, even in the Nimonic 105. These sulfides formed, in spite of the formation of continuous aluminum oxide or chromium-oxide outer scales, which became protective from an oxidation point of view. This result agrees with earlier findings documented in the literature, which state that "protective" oxide films do not prevent the diffusion of sulfur into the metal and subsequent formation of internal sulfides.

The partial success with the Nimonic alloy in previous work led to the testing of Kanthal A-1 and Cabot 214. That approach was to select alloys that had ~5% aluminum, the minimum required for the formation of an outer alumina scale, but no significant alloying additions of the ready sulfide formers such as titanium and manganese. Thus, like Nimonic, an alumina scale would form and prevent further oxidation and oxygen penetration of grain boundaries, but, in contrast to Nimonic, contain no titanium or manganese to react with sulfur to form internal sulfides. The results for Kanthal A-1 agreed with this approach, those for Cabot 214 did not. The reasons for the lack of oxidation resistance of the Cabot 214, and to a lesser degree Nimonic 105, are not fully understood. However, the most probable cause was the absence in the alloys of sufficient chromium to form sequential layers of chromia, particularly when subjected to a cyclic-temperature mode where oxide-scale adherence was compromised. The Kanthal A-1 did form protective outer scale layers of chromia and alumina, which prevented oxygen penetration of grain boundaries. It also did not form a zone of internal sulfides.

DISTRIBUTION:

2500	D. B. Hayes, Actg
2510	D. H. Anderson
2514	L. L. Bonzon
2514	L. J. Weirick (10)
6220	D. G. Schueler
6227	J. A. Leonard
6227	R. B. Diver
6227	J. I. Martinez
6227	J. F. Muir
6227	E. E. Rush
8524	P. W. Dean
3141	S. A. Landenberger (5)
3151	W. L. Garner (3)
3154-1	C. H. Dalin (28)
	For DOE/OSTI (Unlimited Release)